INSTITUTE OF PHYSICS PUBLISHING JOURNAL OF PHYSICS: CONDENSED MATTER

J. Phys.: Condens. Matter **14** (2002) 4915–4925 PII: S0953-8984(02)30357-6

Susceptibility measurements on a fractionated aggregate-free ferrofluid

G A van Ewijk, G J Vroege[1] and A P Philipse

Van't Hoff Laboratory for Physical and Colloid Chemistry, Debye Institute, Utrecht University, Padualaan 8, 3584 CH Utrecht, The Netherlands

E-mail: g.j.vroege@chem.uu.nl

Received 30 October 2001
Published 2 May 2002
Online at stacks.iop.org/JPhysCM/14/4915

Abstract

The concentration dependence of the susceptibility of aggregate-free ferrofluids was investigated. The ferrofluids consisted of oleic-acid-grafted magnetite particles in cyclohexane. One of the samples contained strongly interacting particles (interaction strength of approximately $5kT$). Qualitatively, the measurements are in agreement with theoretical predictions on dipolar hard-sphere fluids: dipolar interactions raise the susceptibility above the ideal (Langevin) susceptibility, and when plotted as a function of the Langevin (ideal) susceptibility, the measurements on the two samples are very similar. Quantitatively, theoretical predictions overestimate the experimental susceptibilities at higher ferrofluid concentrations.

1. Introduction

The dipolar hard-sphere (DHS) model is the starting point for the theoretical description of polar molecules. Calculating the properties of this model system has proven to be a hard problem. Since Debye published the first paper on the dielectric constant of polar molecules [1] in 1912, several alternative calculations of the dielectric constant have appeared [2–6], some very recently [7–10]. The ongoing debate over presence or absence of a stable gas–liquid equilibrium in DHS fluids [11, 12] illustrates that this system is still not well understood.

Although polar molecules resemble the DHSs in some aspects, they have properties that complicate testing of the predicted dielectric constant against experimental values, such as a non-zero polarizability, a non-spherical shape, and van der Waals interaction. Therefore, ferrofluids [13] have been used instead for direct comparison with theory [14–16]. These colloidal dispersions contain nearly spherical, single-domain magnetic particles. The particles have a permanent magnetic dipole moment, negligible magnetizability, and can be made approximately hard repulsive, thus making them essentially DHSs. Ferrofluids are flexible

[1] Author to whom any correspondence should be addressed.

model systems: the strength of dipolar interaction between the particles can be adjusted by means of their size or the temperature, and their number density can be conveniently modified via the amount of solvent.

The most commonly studied ferrofluid consists of an apolar solvent (typically kerosene) in which magnetite (Fe_3O_4) particles with a typical diameter of 10 nm are dispersed. A monolayer of oleic acid grafted on the surface of these particles prevents massive irreversible agglomeration. Unfortunately, these ferrofluids are always polydisperse: a relative polydispersity of 40% is not uncommon. This property complicates a quantitative comparison of measurements with theoretical predictions, but the polydispersity is at least determined in most studies. A more serious problem is the presence of small irreversible aggregates, the formation of which during synthesis can hardly be prevented (these should not be confused with the chain-like aggregates that may form reversibly due to dipole–dipole attraction). Acting as magnetizable particles, such aggregates can obtain a large dipole moment in a magnetic field and can dominate the magnetic properties of ferrofluids, or, as Scholten [17] put it, 'the colloid becomes a caricature of a magnetic fluid'.

It is the aim of this study to compare susceptibility measurements on *aggregate-free* ferrofluids with theoretical predictions. In one of the ferrofluids, the dipolar interaction strength is about seven times larger than in usual ferrofluids. This sample was obtained by isolating the large particles using size-selective precipitation [18, 19]. The susceptibility is measured at a fixed temperature as a function of concentration over a large concentration range. Corrections and uncertainties associated with temperature-dependent measurements, such as for expansion of the solvent, decrease of the magnetization, and possibly a decline of colloid stability, are thus avoided.

The results of our study show that, firstly, the susceptibilities expressed in terms of the ideal (Langevin) susceptibility are very similar for the two systems, despite their difference in interaction strength. Secondly, all tested theories, except Onsager's theory, overestimate the measured susceptibilities.

2. Theory

If a magnetic field H is applied to a ferrofluid, the magnetic dipole moments m of the magnetic particles tend to align parallel to that field, causing a net magnetization $M = nm\langle\cos\theta\rangle$ with n the particle number density, θ the angle between a magnetic moment and the field, and $\langle\ \rangle$ denoting the thermal average. The initial susceptibility $\chi_i = (\partial M/\partial H)_{H\to 0}$ defines the strength of response to an applied field. In the case of non-interacting dipoles, corresponding to a dilute ferrofluid, the susceptibility is called the 'Langevin susceptibility', χ_L:

$$\chi_L = \frac{\mu_0 n m^2}{3kT}, \tag{1}$$

where μ_0 is the permeability of vacuum and kT the thermal energy.

In ordinary ferrofluids, the dipole–dipole interaction is about $1kT$, which is sufficient to affect the susceptibility of concentrated ferrofluids. Accounting for dipolar interactions is a long-standing problem, which was studied as early as 1907 by Weiss [20] to explain ferromagnetism and the existence of the Curie temperature. His theory is based on the idea that each dipole experiences an effective field H, which is composed of the externally applied field H_0 plus a field κM due to all other dipoles. In liquids, the value of κ is determined by the shape of the imaginary cavity in which each dipole is thought to reside. The susceptibility according to this model is

$$\chi_i = \frac{\chi_L}{1 - \kappa\chi_L} \tag{2}$$

where χ_L is given by (1). For a spherical cavity, κ is 1/3. A result equivalent to (2) was obtained by Debye in 1912 for the dielectric constant of polar materials [1] (because electric and magnetic dipoles are analogous, expressions for the dielectric constant ε can be translated to ones for its magnetic counterpart, the magnetic permeability $\mu = \chi + 1$).

According to (2), χ_i diverges at $\chi_L \to 3$, a phenomenon observed neither in dielectric materials nor in ferrofluids. By decomposing the effective field into a 'cavity field' parallel to the external field and a 'reaction field' parallel to the central dipole, Onsager was able to show that the predicted spontaneous polarization is a result from the incorrect assumption that the reaction field exerts a torque on the central dipole [2]. In Onsager's theory, divergence of the dielectric constant is absent, in accordance with experience. The susceptibility following from this model is

$$\chi_i = \tfrac{3}{4}\Big(\chi_L - 1 + \sqrt{1 + \tfrac{2}{3}\chi_L + \chi_L^2}\Big). \tag{3}$$

Kirkwood later generalized Onsager's theory [3], and Wertheim solved Kirkwood's result within the mean-spherical model (MSM) [4]. The susceptibility within the MSM is

$$\chi_i = \frac{q(2\xi) - q(-\xi)}{q(-\xi)}; \qquad q(\xi) = \frac{(1+2\xi)^2}{(1-\xi)^4} \tag{4}$$

where the parameter ξ can be found by solving $\chi_L = q(2\xi) - q(-\xi)$.

More recently, perturbation theories have gained in interest. These theories are based on expansion of the free energy in the volume fraction $\phi = n(\pi/6)d^3$ (d is the particle diameter) and/or dimensionless interaction strength $\lambda = \mu_0 m^2/(4\pi kTd^3)$. The first (exact) terms of the expansion are [8, 9, 21, 22]

$$\chi_i \approx \chi_L + \tfrac{1}{3}\chi_L^2 + \tfrac{1}{144}\chi_L^3 + \cdots. \tag{5}$$

The linear and quadratic term in (5) can also be found by expanding any of the expressions for χ_i described in this section in terms of χ_L. The correct cubic term is only obtained from the MSM.

Note that, although interaction strength and concentration are independent, they appear only as the single, combined variable $\chi_L = 8\phi\lambda$ in equations (2)–(5). Expansions to higher orders give expressions which depend on ϕ and λ separately [7–10, 22].

3. Experimental procedure

3.1. Ferrofluids and fractionation

A high-quality ferrofluid, called FFR, was fractionated by size-selective precipitation, using pentanol as a bad solvent. This ferrofluid consisted of Fe_3O_4 colloids, grafted with purified oleic acid and dispersed in cyclohexane of analytical purity. Unreacted oleic acid was removed by repeated precipitation and redispersion. Clustered particles were removed by magnetic filtration.

In the first fractionation step, FFR with a particle concentration of about 10% by volume was partially destabilized by stepwise addition of pentanol. After each addition, the sample was ultrasonicated for 5 min and left undisturbed for at least 4 h to let aggregates settle. The supernatant was separated from the sediment when the magnetic susceptibility of the supernatant indicated that about half of the particles were flocculated. Both the sediment and the supernatant, called FFR-S and FFR-L respectively, were fractionated once more by adding pentanol or cyclohexane.

Pentanol was removed by precipitating and washing all four fractions with ethanol. After drying in a dry nitrogen stream, the products were redispersed in cyclohexane.

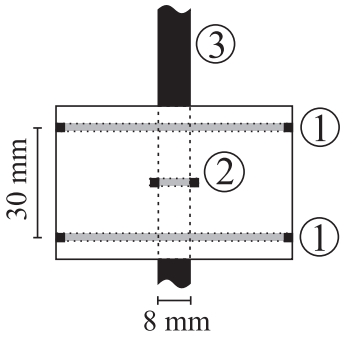

Figure 1. A schematic drawing of one transformer. (1) Helmholtz coils, generating a homogeneous magnetic field of 100 A m^{-1}; (2) a secondary coil, measuring χ_i; (3) the sample tube. The susceptibility meter contains two identical transformers of this kind.

3.2. Characterization

The physical diameter of the core of Fe_3O_4 particles, d_c, was obtained from transmission electron microscopy pictures, taken on a Philips CM10 microscope, and analysed with IBAS, an electronic image analysis system.

Magnetization measurements were performed on a MicroMag 2900 AGM (Alternating Gradient Magnetometer, Princeton Measurements Corp.). Samples were contained in small glass cups with internal dimensions of 4 × 3 × 0.4 mm, which were sealed by gluing a small cover glass over the open end. All measurements were performed at room temperature. The saturation magnetization and diamagnetic susceptibility were determined by fitting the magnetization curve at high fields (up to 1.2×10^6 A m^{-1}) with the Langevin function [13,23] and an added diamagnetic contribution:

$$M = M_s \left\{ \coth(\alpha) - \frac{1}{\alpha} \right\} + \chi_{dia} H; \qquad \alpha = \frac{\mu_0 m H}{kT} \tag{6}$$

where M_s is the saturation magnetization of the sample, χ_{dia} the diamagnetic susceptibility, H the applied field strength, m the magnetic moment of particles, μ_0 the permeability of vacuum, and kT the thermal energy. The initial susceptibility χ_i was calculated from magnetization data at applied fields below 10^3 A m^{-1}. These points invariably lie on a straight line. The magnetic core size of particles was calculated using the low-field approximation of (6):

$$\chi_i = M_s \frac{\mu_0 m}{3kT} + \chi_{dia} = M_s \frac{\mu_0 M_{s,Fe_3O_4} \pi d_M^3}{18kT} + \chi_{dia} \tag{7}$$

with M_{s,Fe_3O_4} the saturation magnetization of bulk Fe_3O_4 (4.8×10^5 A m^{-1}) and d_M the magnetic core diameter. To minimize the influence of magnetic interaction between magnetite particles, equation (7) was only used for measurements on dilute samples, having a concentration of magnetic material below 10 g l^{-1}. It should be noted that the diameter d_M can deviate significantly from the physical diameter d_c obtained with TEM. One reason is that d_M^3 actually equals $\langle d_m^6 \rangle / \langle d_m^3 \rangle$ [24, 25] (d_m is the core size of one particle), so polydispersity strongly increases the diameter found with (7). A second reason is that the surface of particles may be non-magnetic [13, 25].

Small-angle x-ray scattering (SAXS) experiments were carried out at the DUBBLE beamline (BM26) at the European Synchrotron Radiation Facility in Grenoble. Scattering experiments were conducted on dilute samples ($\phi < 1\%$). The radius of gyration, R_g, was calculated using the low-q approximation of the scattering intensity of a dilute dispersion [26]:

$\ln[I(q)/I(0)] = -R_g^2 q^2/3$, where $q = (4\pi n/\lambda_0)\sin(\theta/2)$ is the scattering vector, θ is the scattering angle and $\lambda_0 = 1.03$ Å the wavelength of incident radiation.

The mass density ρ of a dispersion was measured with an DMA 5000 densitometer (Anton Paar). Combined with the mass concentration c this yields the density of dry particles ρ_{dry}:

$$\rho_{dry} = \frac{c\rho_{solvent}}{c + \rho_{solvent} - \rho}, \tag{8}$$

which is used to calculate volume fractions of samples with known weight concentration.

3.3. Susceptibility measurements

The concentration dependence of the susceptibility was measured on a Kappabridge KLY-3 susceptibility meter (Agico). The KLY-3 applies a homogeneous field of 300 A m^{-1}, oscillating at a frequency of 875 Hz. All measurements were done at 296.65 ± 0.2 K.

Ferrofluid samples were contained in 300 μl cylindrical glass tubes with a length/diameter ratio of 9. With the field applied along the long axis of the sample, demagnetization effects [27] can be neglected, as was experimentally confirmed by measuring samples with higher length/diameter ratios. It was also verified that the instrument's read-out value depends linearly on the susceptibility of the sample. And finally, the susceptibility was measured for eleven dilute samples of FFR with $\chi_i < 2$. This curve should follow $\chi_i = \chi_L(1+\chi_L/3)$, regardless of particle shape or polydispersity, because the radial distribution function at low concentrations is spherically symmetric (hence the factor 1/3) and the same for each kind of particle.

The concentration-dependent susceptibility of FFR-LL was also measured in a home-made set-up using two transformers of the type shown in figure 1. Each transformer consists of two coils in the Helmholtz configuration and one small, thin pickup coil, positioned halfway between the Helmholtz coils. The Helmholtz coils generate a homogeneous magnetic field of 100 A m^{-1}, oscillating at a frequency of 875 Hz. The oscillating field produces an oscillating voltage difference over the pickup coil. The pickup signal is compensated by a second (reference) transformer, and measured with a lock-in amplifier. When a sample tube is inserted in one of the pickup coils, the resulting voltage difference over the two pickup coils is proportional to the susceptibility of the sample.

In this 'balanced transformer' set-up, a concentration series was measured by drying some FFR-LL in a long 8 mm wide sample tube under a dry nitrogen stream, and measuring the susceptibility after successive dilutions with cyclohexane. After each dilution, the sample was weighed and left to equilibrate for at least 15 min before the susceptibility was measured. The concentration was calculated afterwards from the weights of dry material and dispersion and the densities of dry material and cyclohexane.

The frequency dependence of the susceptibility was also measured in the balanced transformer set-up. As the susceptibility is measured at approximately 1 kHz, there is the danger that the measured quantity is not equal to the static susceptibility [28]. In fact, a frequency dependence below 1 kHz has been found before for similar ferrofluids [29]. To test whether the same effects can occur in our measurements, the dynamic susceptibility of FFR with a concentration of 1500 g l^{-1} was measured from 10 Hz up to 10 kHz (the limit for our instrument).

4. Results and discussion

4.1. Characterization

Fractionation. Precipitation of FFR started at a pentanol volume fraction of 50% and complete precipitation was found at 90%. These percentages were, however, strongly affected by small temperature variations.

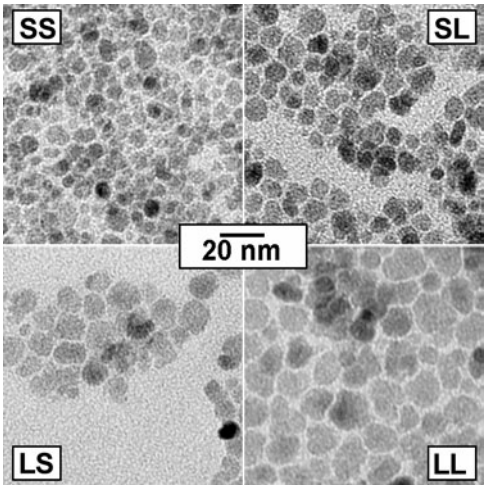

Figure 2. Electron microscopy pictures of the four ferrofluid fractions, shown at the same magnification; see table 1 for details.

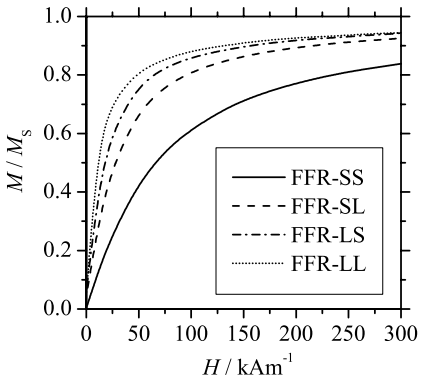

Figure 3. Magnetization measurements of the four ferrofluid fractions. The difference in particle size between samples is evident from the difference in initial slope.

Table 1 shows the characteristics of FFR and the four ferrofluid fractions. Both TEM (figure 2) and magnetization measurements (figure 3) yield significant differences between the mean diameters and hence the maximum strength of dipole–dipole interactions in the fractions. Fraction FFR-LL is especially interesting, for it consists of large particles of a size not reported before. Dipole–dipole interaction can become as strong as $-5.4kT$ in this system. Despite its strong interaction, FFR-LL is stable at volume fractions up to 35%, possibly higher. Conversely, adding cyclohexane to dried FFR-LL does not give an 'instant ferrofluid', not even an immediate coloration of the solvent, whereas cyclohexane instantly becomes black when added to dried samples of the other fractions. For FFR-LL it takes about ten hours before redispersion is complete. Apparently, the strong interaction makes redispersion difficult, but it does not prohibit a stable ferrofluid.

The polydispersity was reduced from 26% (FFR) to 18% (FFR-LL), which is somewhat less than expected. Similar behaviour was found in fractionation studies on aqueous ferrofluids [30, 31], where size sorting resulted in different mean sizes but almost the same

Table 1. Characteristics of ferrofluid and ferrofluid fractions.

Sample	d_c (nm)[a]	σ_c (nm)[a]	d_M (nm)[b]	ρ_{dry} (kg m^{-3})	λ
Unfractionated FFR	9.1	2.3	11.3	2900	0.40
Fraction FFR-SS	7.9	1.3	7.7		0.25
Fraction FFR-SL	9.7	2.6	9.9		0.55
Fraction FFR-LS	11.4	2.8	11.7		1.0
Fraction FFR-LL	15.0	2.8	15.22	3630	2.7

[a] Determined from TEM pictures.
[b] Obtained from magnetization measurements.

polydispersity. Still, the polydispersity of all samples used here is lower than the polydispersity of 40% that is often reported in the literature. The fractionation method described here can perhaps be improved upon by varying the temperature to modify the solvent quality of the pentanol/cyclohexane mixture. In this way, a more gradual and homogeneous precipitation can be achieved, possibly yielding fractions with lower polydispersity.

Aggregation. Figure 4 shows the Guinier plot of a dilute sample of FFR at small scattering vectors. A straight line fits the scattering curve well and gives a radius of gyration of 6.5 nm. For homogeneous spherical particles, the physical diameter is $d = 2R_g\sqrt{5/3} = 16.8$ nm. Because scattering by the grafting layer is negligible, this diameter is that of the iron oxide core. The difference between the SAXS diameter and TEM diameter can be largely attributed to polydispersity. If particle sizes are log-normally distributed, then [24]

$$\frac{d_{SAXS}}{d_{TEM}} = \frac{\sqrt{\langle d^8\rangle/\langle d^6\rangle}}{\langle d\rangle} = \frac{\exp(7\sigma^2)}{\exp(\sigma^2/2)}. \tag{9}$$

Substituting $\sigma = 0.26$ and $\langle d\rangle = 9.1$ (see table 1) in (9) yields $d_{SAXS} = 14.1$ nm. The linearity of the Guinier plot up to the smallest q-value and the fairly good agreement with TEM data clearly demonstrate the absence of a significant number of clusters. This test is even sensitive for small clusters, such as doublets: a doublet containing two particles of diameter d has a radius of gyration of $R_g = \frac{1}{2}d\sqrt{8/5}$, which is 1.63 times as large as R_g for a singlet of the same diameter. A significant number of doublets would therefore lead to a much larger radius than we found here. For triplets and larger clusters, the sensitivity is even higher.

Absence of a sediment in ferrofluid samples is insufficient to allow one to conclude that clusters are absent [17]: sediments only form when the gravitational length [32] $l_g = kT/Nmg$ (N = number of particles in a cluster, m = mass of a single particle, $\approx 3 \times 10^{-21}$ kg (corrected for buoyancy), g = Earth's gravitational constant) is less than, say, a millimetre. This condition is only satisfied for clusters of about 100 particles or more; smaller clusters simply remain dispersed due to their Brownian motion. Moreover, the sedimentation velocity of a 100-particle aggregate is only $u \approx Nmg/[6\pi\eta_0(N^{1/3}d)] = 100\,\mu$m day^{-1}, so sediments of such aggregates take typically months to develop (if they develop at all; sedimentation is easily disturbed by thermal convection).

The absence of clusters is in agreement with dichroism and rheological measurements done with the same kind of ferrofluid [33].

4.2. Susceptibility measurements

Verifications. The low-concentration susceptibility profile of FFR was fitted with the polynomial $\chi_i = kc(1+Qkc)$ with $kc = \chi_L$; c is the concentration, k a proportionality constant, and Q a coefficient which should correspond to the Lorentz factor 1/3 (see (5)). Q was found

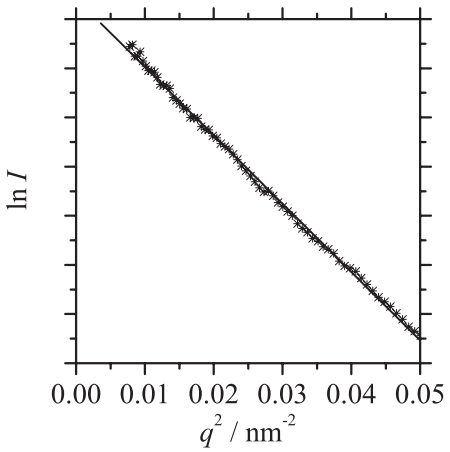

Figure 4. A Guinier plot of the SAXS measurement for diluted ferrofluid. Linearity up to small q and agreement between the Guinier radius and TEM radius, and polydispersity, indicate the absence of aggregates.

to be 0.37 ± 0.06, which agrees with the expected value within experimental accuracy. This also demonstrates that demagnetization effects are negligible (the demagnetization factor can be simply calculated as $1/3 - Q$).

The susceptibility of the concentrated FFR sample shows no dependence on the frequency up to 10 kHz. This was not surprising, since the relaxation times of magnetic moments in this ferrofluid are orders of magnitudes smaller than 10^{-4} s, even for the larger particles. Consider, for example, a particle with a diameter of 20 nm (including the oleic-acid layer). In a dilute ferrofluid, it will have a Brownian relaxation time [13] $\tau_B = \pi d^3 \eta_0/(2kT) = 3 \times 10^{-6}$ s in a solvent with a viscosity $\eta_0 = 10^{-3}$ Pa s. Increasing the concentration will slow down rotation, but studies on the rotational diffusion of hard spheres show that this increase in relaxation time is only by a factor of about three. Relaxation times much longer than those calculated here can only be expected for large particles (with long Néel relaxation times) which are part of an aggregate. This point was also put forward in [34], and even used to measure the sizes of aggregates.

Susceptibility curves. For the samples FFR and FFR-LL, susceptibility measurements are shown in figure 5. The ordinate values χ_L were calculated from the concentration c with $\chi_L = kc$, where the proportionality constant k was obtained by fitting measurements on dilute samples with the low-concentration expansion $\chi_i = \chi_L(1+\chi_L/3)$. This approximation differs by less than 2% from the exact values at $\chi_L < 0.3$. In figure 5(b), the k obtained from the balanced transformer data was also used to rescale the Kappabridge data. The proportionality constants for FFR and FFR-LL are $k = 4.70$ and 18.6 m^3 kg^{-1}, respectively.

The volume fraction ϕ, calculated from the mass concentration c and the density ρ_{dry} (table 1), is also shown in the graphs. Note that ϕ is only an approximation of the true volume fraction, since it is obtained from the density of dry material.

The concentration dependent susceptibility of FFR-LL is of particular interest, because the polydispersity in particle sizes is relatively low and the mean magnetic dipole moment (and hence also dipole–dipole interaction) is very high for Fe_3O_4-based ferrofluids. Despite the significant difference in particle size and dipolar interaction strength, the susceptibility curves

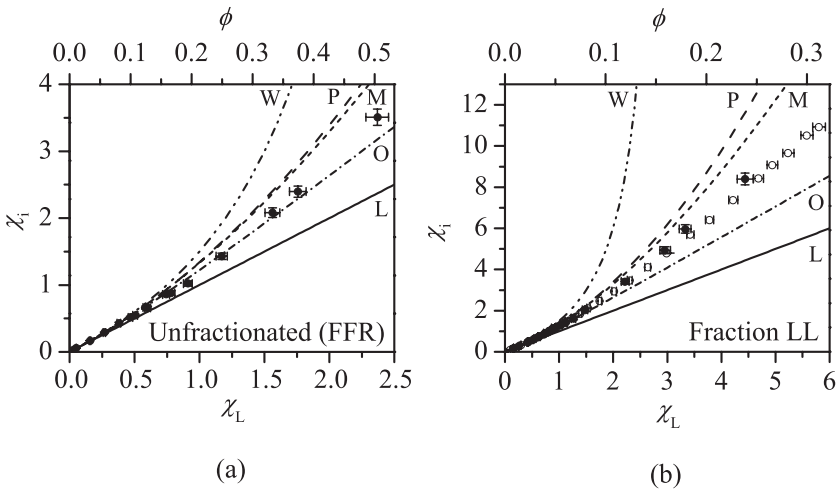

Figure 5. Concentration-dependent susceptibilities of (*a*) the unfractionated ferrofluid and (*b*) fraction LL, containing the strongly interacting particles. Solid symbols indicate measurements taken with the Kappabridge, open symbols ones taken with the balanced transformer. The lines denote different theoretical curves (L: Langevin; O: Onsager; M: MSM; P: Perturbation theory; W: Weiss).

of FFR and FFR-LL plotted as a function of χ_L (figures 5(*a*) and (*b*)) are very similar: the maximum relative difference in χ_i between the two curves amounts to 14%. This dependence of χ_i on χ_L alone is also seen in equations (2)–(5).

As expected, dipolar interactions lead to non-Langevin behaviour at high concentrations (figure 5). However, none of the theories described in section 2 appears to describe our data very well. Surprisingly, the MSM overestimates our results, while the MSM probably gives an underestimate of the true susceptibility (for DHS fluids) [7]. This is also supported by Monte Carlo simulation results [35], though it should be noted that obtaining accurate susceptibilities from simulations has proven to be a very hard problem [36].

Our results are in disagreement with previous conclusions that the concentration-dependent susceptibility of oleic-acid/magnetite ferrofluids is well described by the MSM [15, 28, 37]. We cannot account for this discrepancy, but speculatively ascribe it to a difference in degree of aggregation (in a subsequent paper reporting a detailed study of aggregation, the same author found that in similarly prepared ferrofluids, about half of the particles are present in irreversible aggregates [34]). Interestingly, Fannin *et al* [16] seem to find a similar discrepancy: they report that the slope of the susceptibility curve increases with increasing concentration, but at a lower rate than reported in [37].

The experimental curve of FFR (figure 5(*a*)) seems to be well described by a second-order polynomial in the concentration c, $\chi_i = kc(1 + Qkc)$, with the quadratic coefficient $Q = 0.160 \pm 0.024$. However, the scale misleads the eye: the curve at low concentrations is best described with $Q = 0.37 \pm 0.06$, as was already mentioned. Still, because the influence of the quadratic term is small at low concentrations, the data in this regime are not very sensitive to the exact value of Q, so $Q = 0.160$ also describes the data reasonably well.

For the description of FFR-LL (figure 5(*b*)), inclusion of the cubic term is essential. This can be seen in figure 6, where χ_i/c is plotted against c. The curve is clearly non-linear; hence a fit of χ_i with a quadratic function is not adequate. The susceptibility of FFR-LL follows the function $\chi_i = kc(1 + Qkc + Ck^2c^2)$ with $Q = 0.235 \pm 0.004$ and $C = -0.0160 \pm 0.0006$. The sign of the coefficient C does not correspond to that of the

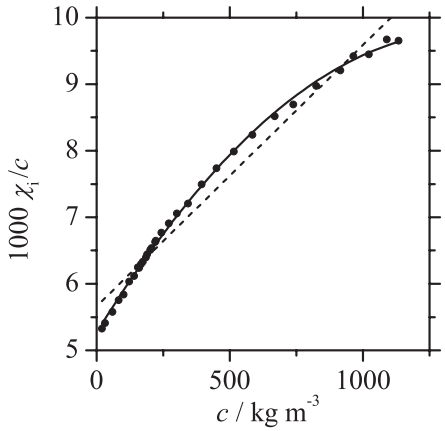

Figure 6. Susceptibility measurements on FFR-LL. The data in this representation are better described by a parabolic function (solid curve) than by a straight line (dashed line), meaning that a polynomial formula for $\chi_i(c)$ should include a c^3-term.

perturbation theories, e.g. equation (5), but in the parametrized dielectric constant according to the linearized hypernetted chain (LHNC) approximation [38], the cubic coefficient is negative.

5. Conclusions

In this paper, concentration-dependent susceptibility measurements on two aggregate-free ferrofluids were discussed. The ferrofluids consisted of oleic-acid-grafted magnetite particles in cyclohexane. Although the strengths of interaction were significantly different for the two samples (approximately $1kT$ and $5kT$), the susceptibility curves plotted as a function of the Langevin susceptibility were very similar. Such behaviour is in accordance with most theories.

At higher concentrations, the curves deviated from theoretical curves according to perturbation theory, the MSM, and Onsager's theory. The concentration-dependent susceptibility of the sample with the weakest interaction could be well described by a second-order polynomial. For the sample with strongly interacting particles, a second-order polynomial was not adequate: inclusion of the cubic term was shown to be necessary.

Although the data were compared with different theories in this paper, this should not be seen as a rigorous test for those theories. We tend to conclude that magnetite-based ferrofluids are not suitable for this purpose, because the particles are somewhat non-spherical (especially the larger ones) and polydisperse, whereas monodisperse spheres are considered in theories. In principle, theories could be adapted for polydispersity; at low concentrations, the effect of polydispersity can be readily incorporated into, for example, perturbation theories. However, just in the regions where the non-ideality of the susceptibility becomes significant, accounting for polydispersity is much more difficult. Rather than adapting the various theories to the shortcomings of the experimental 'model' system, we would like to encourage experimentalists to do similar studies on other types of ferrofluid which resemble the monodisperse DHS fluid more. Although the polydispersity of magnetite-based ferrofluids can be reduced, as shown in this paper, it is still significant. Moreover, the problem of the irregular shape of these particles remains. A better candidate for an experimental system to be used for testing DHS theories would be cobalt-based ferrofluid [39,40]. Despite the drawback of being susceptible to oxidation, cobalt colloids have the advantage of being truly spherical, having a low polydispersity (between 5 and 10%) and a better-tunable dipolar interaction strength.

Acknowledgments

We thank Bonny Kuipers for building the balanced transformer set-up, and Dr B Huke and Dr P Fannin for discussions.

References

[1] Debye P 1912 *Z. Phys.* **13** 97
[2] Onsager L 1936 *J. Am. Chem. Soc.* **58** 1486
[3] Kirkwood J G 1939 *J. Chem. Phys.* **7** 911
[4] Wertheim M S 1971 *J. Chem. Phys.* **55** 4291
[5] Rushbrooke G S, Stell G and Høye J S 1973 *Mol. Phys.* **26** 1199
[6] Tani A, Henderson D, Barker J A and Hecht C E 1983 *Mol. Phys.* **48** 863
[7] Kalikmanov V I 1999 *Phys. Rev.* E **59** 4085
[8] Szalai I, Chan K-Y and Henderson D 2000 *Phys. Rev.* E **62** 8846
[9] Kalikmanov V I 2000 *Phys. Rev.* E **62** 8851
[10] Huke B and Lücke M 2000 *Phys. Rev.* E **62** 6875
[11] Teixeira P I C, Tavares J M and Telo da Gama M M 2000 *J. Physique* **12** R411
[12] Tlusty T and Safran S A 2000 *Science* **290** 1328
[13] Rosensweig R E 1985 *Ferrohydrodynamics* (Cambridge: Cambridge University Press)
[14] Dikanskii Y I 1982 *Magnetohydrodynamics* **18** 237
[15] Pshenichnikov A F, Lebedev A V and Morozov K I 1987 *Magnetohydrodynamics* **23** 31
[16] Fannin P C, Scaife B K P and Charles S W 1990 *J. Phys. D: Appl. Phys.* **23** 1711
[17] Scholten P C 1988 *Chem. Eng. Commun.* **67** 331
[18] Murray C B, Norris D J and Bawendi M G 1993 *J. Am. Chem. Soc.* **115** 8706
[19] van Ewijk G A 2001 Phase behaviour of mixtures of magnetic colloids and non-adsorbing polymer *PhD Thesis* Utrecht University
[20] Weiss P 1907 *J. Physique Radium* **4** 661
[21] Rushbrooke G S 1979 *Mol. Phys.* **37** 761
[22] Ivanov A O and Kuznetsova O B 2001 *Colloid J.* **63** 64
[23] Jacobs I S and Bean C P 1963 *Magnetism, a Treatise on Modern Theory and Materials* vol 3, ed G T Rado *et al* (New York: Academic) p 271
[24] Cabuil V and Perzynski R 1996 *Magnetic Fluids and Applications Handbook* ed B Berkovski (New York: Begell House)
[25] Pshenichnikov A F, Mekhonoshin V V and Lebedev A V 1996 *J. Magn. Magn. Mater.* **161** 94
[26] Porod G 1982 *Small Angle X-Ray Scattering* ed O Glatter *et al* (London: Academic) p 17
[27] Dijkstra H 1967 *Selected Topics in Solid State Physics* ed E P Wohlfarth (Amsterdam: North-Holland)
[28] Pshenichnikov A F 1995 *J. Magn. Magn. Mater.* **145** 319
[29] Maiorov M M 1979 *Magnetohydrodynamics* **2** 135
[30] Cabuil V, Massart R, Bacri J-C, Perzynski R and Salin D 1987 *J. Chem. Res. (Suppl.)* 130
[31] Bacri J-C, Perzynski R, Salin D, Cabuil V and Massart R 1988 *J. Colloid Interface Sci.* **132** 43
[32] Degiorgio V, Piazza R and Bellini T 1995 *Observation, Prediction and Simulation of Phase Transitions in Complex Fluids* ed M Baus *et al* (Dordrecht: Kluwer)
[33] Vékás L, Rasa M and Bica D 2000 *J. Colloid Interface Sci.* **231** 247
[34] Buzmakov V M and Pshenichnikov A F 1996 *J. Colloid Interface Sci.* **182** 63
[35] Patey G N, Levesque D and Weis J J 1982 *Mol. Phys.* **45** 733
[36] de Leeuw S W, Perram J W and Smith E R 1986 *Annu. Rev. Phys. Chem.* **37** 245
[37] Morozov K I, Pshenichnikov A F, Raikher Y L and Shliomis M I 1987 *J. Magn. Magn. Mater.* **65** 269
[38] Patey G N, Levesque D and Weis J J 1979 *Mol. Phys.* **38** 219
[39] Papirer E, Horny P, Balard H, Anthore R, Pepitas C and Martinet A 1983 *J. Colloid Interface Sci.* **94** 207
[40] Pathmamanoharan C and Philipse A P 1998 *J. Colloid Interface Sci.* **205** 340